EUROPEAN ORGANIZATION FOR NUCLEAR RESEARCH

CERN-PPE/92-48
26 March 1992

Measurement of B-$\bar{\text{B}}$ Mixing at the Z using a Jet-Charge Method

The ALEPH Collaboration[1]

Abstract

Results on $B^0 - \bar{B}^0$ mixing in e^+e^- annihilation at LEP are reported. A new method is used, where the charge of one b quark is tagged by a high-p, high-$p_\perp$ electron or muon, and the charge of the other is extracted from the momentum-weighted average of the charges of jet fragments. Based on the analysis of 180,000 hadronic Z decays produced in the ALEPH detector, $f_d\chi_d + 0.72 f_s\chi_s = 0.113 \pm 0.018\,(\text{stat.}) \pm 0.027\,(\text{syst.})$ is obtained. Combining this result with the ALEPH dilepton measurement yields $\chi = 0.129 \pm 0.022$.

(Submitted to Physics Letters B)

[1]See the following pages for the list of authors.

B. Bloch-Devaux, P. Colas, W. Kozanecki,[2] M.C. Lemaire, E. Locci, S. Loucatos, E. Monnier, P. Perez, F. Perrier, J. Rander, J.-F. Renardy, A. Roussarie, J.-P. Schuller, J. Schwindling, D. Si Mohand, B. Vallage

Service de Physique des Particules, DAPNIA, CE-Saclay, 91191 Gif-sur-Yvette Cedex, France[18]

R.P. Johnson, A.M. Litke, J. Wear

Institute for Particle Physics, University of California at Santa Cruz, Santa Cruz, CA 95064, USA

J.G. Ashman, W. Babbage, C.N. Booth, C. Buttar, R.E. Carney, S. Cartwright, F. Combley, F. Hatfield, P. Reeves, L.F. Thompson

Department of Physics, University of Sheffield, Sheffield S3 7RH, United Kingdom[11]

E. Barberio, S. Brandt, C. Grupen, L. Mirabito,[31] U. Schäfer, H. Seywerd

Fachbereich Physik, Universität Siegen, 5900 Siegen, Fed. Rep. of Germany[17]

G. Ganis,[35] G. Giannini, B. Gobbo, F. Ragusa[24]

Dipartimento di Fisica, Università di Trieste e INFN Sezione di Trieste, 34127 Trieste, Italy

L. Bellantoni, D. Cinabro,[34] J.S. Conway, D.F. Cowen,[23] Z. Feng, D.P.S. Ferguson, Y.S. Gao, J. Grahl, J.L. Harton, R.C. Jared,[7] B.W. LeClaire, C. Lishka, Y.B. Pan, J.R. Pater, Y. Saadi, V. Sharma, M. Schmitt, Z.H. Shi, Y.H. Tang, A.M. Walsh, F.V. Weber, M.H. Whitney, Sau Lan Wu, X. Wu, G. Zobernig

Department of Physics, University of Wisconsin, Madison, WI 53706, USA[12]

[†] Deceased.

[1] Now at CERN, PPE Division, 1211 Geneva 23, Switzerland.

[2] Permanent adddress: SLAC, Stanford, CA 94309, USA.

[3] Permanent address: University of Washington, Seattle, WA 98195, USA.

[4] Now at SSCL, Dallas, TX, U.S.A.

[5] Also Istituto di Fisica Generale, Università di Torino, Torino, Italy.

[6] Also Istituto di Cosmo-Geofisica del C.N.R., Torino, Italy.

[7] Permanent address: LBL, Berkeley, CA 94720, USA.

[8] Supported by CICYT, Spain.

[9] Supported by the National Science Foundation of China.

[10] Supported by the Danish Natural Science Research Council.

[11] Supported by the UK Science and Engineering Research Council.

[12] Supported by the US Department of Energy, contract DE-AC02-76ER00881.

[13] Supported by the US Department of Energy, contract DE-FG05-87ER40319.

[14] Supported by the NSF, contract PHY-8451274.

[15] Supported by the US Department of Energy, contract DE-FC0S-85ER250000.

[16] Supported by SLOAN fellowship, contract BR 2703.

[17] Supported by the Bundesministerium für Forschung und Technologie, Fed. Rep. of Germany.

[18] Supported by the Direction des Sciences de la Matière, C.E.A.

[19] Supported by Fonds zur Förderung der wissenschaftlichen Forschung, Austria.

[20] Supported by the Korean Science and Engineering Foundation and Ministry of Education.

[21] Supported by the World Laboratory.

[22] On leave of absence from MIT, Cambridge, MA 02139, USA.

[23] Now at California Institute of Technology, Pasadena, CA 91125, USA.

[24] Now at Dipartimento di Fisica, Università di Milano, Milano, Italy.

[25] Also at CERN, PPE Division, 1211 Geneva 23, Switzerland.

[26] Now at DESY, Hamburg, Germany.

[27] Now at University of California at Santa Barbara, Santa Barbara, CA 93106, USA.

[28] Also at Dipartimento di Fisica, Università di Trieste, Trieste, Italy.

[29] Now at INFN, Pavia, Italy.

[30] Now at Lufthansa, Hamburg, Germany.

[31] Now at Institut de Physique Nucléaire de Lyon, 69622 Villeurbanne, France.

[32] Also at Università di Napoli, Dipartimento di Scienze Fisiche, Napoli, Italy.

[33] On leave of absence from IHEP, Beijing, The People's Republic of China.

[34] Now at Harvard University, Cambridge, MA 02138, U.S.A.

[35] Supported by the Consorzio per lo Sviluppo dell'Area di Ricerca, Trieste, Italy.

The ALEPH Collaboration

D. Buskulic, D. Decamp, C. Goy, J.-P. Lees, M.-N. Minard, B. Mours

Laboratoire de Physique des Particules (LAPP), IN^{2}P^3-CNRS, 74019 Annecy-le-Vieux Cedex, France

R. Alemany, F. Ariztizabal, P. Comas, J.M. Crespo, M. Delfino, E. Fernandez, V. Gaitan, Ll. Garrido, Ll.M. Mir, A. Pacheco, A. Pascual

Institut de Fisica d'Altes Energies, Universitat Autonoma de Barcelona, 08193 Bellaterra (Barcelona), Spain[8]

D. Creanza, M. de Palma, A. Farilla, G. Iaselli, G. Maggi, M. Maggi, S. Natali, S. Nuzzo, M. Quattromini, A. Ranieri, G. Raso, F. Romano, F. Ruggieri, G. Selvaggi, L. Silvestris, P. Tempesta, G. Zito

INFN Sezione di Bari e Dipartimento di Fisica dell' Università, 70126 Bari, Italy

Y. Gao, H. Hu,[21] D. Huang, X. Huang, J. Lin, J. Lou, C. Qiao,[21] T. Wang, Y. Xie, D. Xu, R. Xu, J. Zhang, W. Zhao

Institute of High-Energy Physics, Academia Sinica, Beijing, The People's Republic of China[9]

W.B. Atwood,[2] L.A.T. Bauerdick,[26] E. Blucher, G. Bonvicini, F. Bossi, J. Boudreau, T.H. Burnett,[3] H. Drevermann, R.W. Forty, R. Hagelberg, S. Haywood, J. Hilgart, R. Jacobsen, B. Jost, J. Knobloch, E. Lançon, I. Lehraus, T. Lohse, A. Lusiani, M. Martinez, P. Mato, T. Mattison, H. Meinhard, S. Menary,[27] T. Meyer, A. Minten, A. Miotto, R. Miquel, H.-G. Moser, J. Nash, P. Palazzi, J.A. Perlas, F. Ranjard, G. Redlinger, L. Rolandi,[28] A. Roth,[30] J. Rothberg,[3] T. Ruan,[21,33] M. Saich, D. Schlatter, M. Schmelling, F. Sefkow, W. Tejessy, H. Wachsmuth, W. Wiedenmann, T. Wildish, W. Witzeling, J. Wotschack

European Laboratory for Particle Physics (CERN), 1211 Geneva 23, Switzerland

Z. Ajaltouni, F. Badaud, M. Bardadin-Otwinowska, A.M. Bencheikh, R. El Fellous, A. Falvard, P. Gay, C. Guicheney, P. Henrard, J. Jousset, B. Michel, J-C. Montret, D. Pallin, P. Perret, B. Pietrzyk, J. Proriol, F. Prulhière, G. Stimpfl

Laboratoire de Physique Corpusculaire, Université Blaise Pascal, IN^{2}P^3-CNRS, Clermont-Ferrand, 63177 Aubière, France

T. Fearnley, J.D. Hansen, J.R. Hansen, P.H. Hansen, R. Møllerud, B.S. Nilsson

Niels Bohr Institute, 2100 Copenhagen, Denmark[10]

I. Efthymiopoulos, A. Kyriakis, E. Simopoulou, A. Vayaki,[1] K. Zachariadou

Nuclear Research Center Demokritos (NRCD), Athens, Greece

J. Badier, A. Blondel, G. Bonneaud, J.C. Brient, G. Fouque, A. Gamess, J. Harvey, S. Orteu, A. Rosowsky, A. Rougé, M. Rumpf, R. Tanaka, H. Videau

Laboratoire de Physique Nucléaire et des Hautes Energies, Ecole Polytechnique, IN^{2}P^3-CNRS, 91128 Palaiseau Cedex, France

D.J. Candlin, M.I. Parsons, E. Veitch

Department of Physics, University of Edinburgh, Edinburgh EH9 3JZ, United Kingdom[11]

L. Moneta, G. Parrini

Dipartimento di Fisica, Università di Firenze, INFN Sezione di Firenze, 50125 Firenze, Italy

M. Corden, C. Georgiopoulos, M. Ikeda, J. Lannutti, D. Levinthal,[16] M. Mermikides†, L. Sawyer, S. Wasserbaech

Supercomputer Computations Research Institute and Dept. of Physics, Florida State University, Tallahassee, FL 32306, USA [13,14,15]

A. Antonelli, R. Baldini, G. Bencivenni, G. Bologna,[5] P. Campana, G. Capon, F. Cerutti, V. Chiarella, B. D'Ettorre-Piazzoli,[32] G. Felici, P. Laurelli, G. Mannocchi,[6] F. Murtas, G.P. Murtas, L. Passalacqua, M. Pepe-Altarelli, P. Picchi[5]

Laboratori Nazionali dell'INFN (LNF-INFN), 00044 Frascati, Italy

B. Altoon, O. Boyle, P. Colrain, I. ten Have, J.G. Lynch, W. Maitland, W.T. Morton, C. Raine, J.M. Scarr, K. Smith, A.S. Thompson, R.M. Turnbull

Department of Physics and Astronomy, University of Glasgow, Glasgow G12 8QQ,United Kingdom[11]

B. Brandl, O. Braun, R. Geiges, C. Geweniger, P. Hanke, V. Hepp, E.E. Kluge, Y. Maumary, A. Putzer, B. Rensch, A. Stahl, K. Tittel, M. Wunsch

Institut für Hochenergiephysik, Universität Heidelberg, 6900 Heidelberg, Fed. Rep. of Germany[17]

A.T. Belk, R. Beuselinck, D.M. Binnie, W. Cameron, M. Cattaneo, D.J. Colling, P.J. Dornan,[1] S. Dugeay, A.M. Greene, J.F. Hassard, N.M. Lieske, S.J. Patton, D.G. Payne, M.J. Phillips, J.K. Sedgbeer, G. Taylor, I.R. Tomalin, A.G. Wright

Department of Physics, Imperial College, London SW7 2BZ, United Kingdom[11]

P. Girtler, D. Kuhn, G. Rudolph

Institut für Experimentalphysik, Universität Innsbruck, 6020 Innsbruck, Austria[19]

C.K. Bowdery, T.J. Brodbeck, A.J. Finch, F. Foster, G. Hughes, D. Jackson, N.R. Keemer, M. Nuttall, A. Patel, T. Sloan, S.W. Snow, E.P. Whelan

Department of Physics, University of Lancaster, Lancaster LA1 4YB, United Kingdom[11]

T. Barczewski, K. Kleinknecht, J. Raab, B. Renk, S. Roehn, H.-G. Sander, H. Schmidt, F. Steeg, S.M. Walther, B. Wolf

Institut für Physik, Universität Mainz, 6500 Mainz, Fed. Rep. of Germany[17]

J-J. Aubert, C. Benchouk, V. Bernard, A. Bonissent, J. Carr, P. Coyle, J. Drinkard, F. Etienne, S. Papalexiou, P. Payre, Z. Qian, D. Rousseau, P. Schwemling, M. Talby

Centre de Physique des Particules, Faculté des Sciences de Luminy, IN^2P^3-CNRS, 13288 Marseille, France

S. Adlung, H. Becker, W. Blum,[1] D. Brown, P. Cattaneo,[29] G. Cowan, B. Dehning, H. Dietl, F. Dydak,[25] M. Fernandez-Bosman, M. Frank, A.W. Halley, T. Hansl-Kozanecka,[2,22] J. Lauber, G. Lütjens, G. Lutz, W. Männer, Y. Pan, R. Richter, H. Rotscheidt, J. Schröder, A.S. Schwarz, R. Settles, U. Stierlin, U. Stiegler, R. St. Denis, M. Takashima,[4] J. Thomas,[4] G. Wolf

Max-Planck-Institut für Physik und Astrophysik, Werner-Heisenberg-Institut für Physik, 8000 München, Fed. Rep. of Germany[17]

V. Bertin, J. Boucrot, O. Callot, X. Chen, A. Cordier, M. Davier, J.-F. Grivaz, Ph. Heusse, P. Janot, D.W. Kim,[20] F. Le Diberder, J. Lefrançois,[1] A.-M. Lutz, M.-H. Schune, J.-J. Veillet, I. Videau, Z. Zhang, F. Zomer

Laboratoire de l'Accélérateur Linéaire, Université de Paris-Sud, IN^2P^3-CNRS, 91405 Orsay Cedex, France

D. Abbaneo, S.R. Amendolia, G. Bagliesi, G. Batignani, L. Bosisio, U. Bottigli, C. Bradaschia, M. Carpinelli, M.A. Ciocci, R. Dell'Orso, I. Ferrante, F. Fidecaro,[1] L. Foà, E. Focardi, F. Forti, A. Giassi, M.A. Giorgi, F. Ligabue, E.B. Mannelli, P.S. Marrocchesi, A. Messineo, F. Palla, G. Rizzo, G. Sanguinetti, J. Steinberger, R. Tenchini, G. Tonelli, G. Triggiani, C. Vannini, A. Venturi, P.G. Verdini, J. Walsh

Dipartimento di Fisica dell'Università, INFN Sezione di Pisa, e Scuola Normale Superiore, 56010 Pisa, Italy

J.M. Carter, M.G. Green, P.V. March, T. Medcalf, I.S. Quazi, J.A. Strong, L.R. West

Department of Physics, Royal Holloway & Bedford New College, University of London, Surrey TW20 OEX, United Kingdom[11]

D.R. Botterill, R.W. Clifft, T.R. Edgecock, M. Edwards, S.M. Fisher, T.J. Jones, P.R. Norton, D.P. Salmon, J.C. Thompson

Particle Physics Dept., Rutherford Appleton Laboratory, Chilton, Didcot, Oxon OX11 OQX, United Kingdom[11]

1 Introduction

In the Standard Model the mixing rates of B_d and B_s mesons depend on the mass and weak couplings of the top quark. Existing measurements of B_d mixing on the $\Upsilon(4S)$ resonance [1] and of the combined effect of B_d and B_s mixing at higher energies [2, 3, 4] have provided limits for some of the remaining unmeasured parameters of the CKM matrix that are independent of unitarity assumptions. Most measurements to date of B^0-$\bar{B}^0$ mixing rely on tagging the flavour of both decaying b-hadrons in the event by the charge of their leptonic decay products. These experiments measure the mixing parameter χ, defined as[2]

$$\chi \equiv \frac{\Gamma(b\,\mathrm{hadron} \to \ell^+ X)}{\Gamma(b\,\mathrm{hadron} \to \ell^\pm X)} \tag{1}$$

by comparing the relative abundance of opposite- and equal-sign dileptons.

In this paper, a novel analysis of B^0-$\bar{B}^0$ mixing in hadronic Z decays is performed following recent progress on quark charge tagging using charged particle jets [5]. The b-flavour tagging relies on the selection of events containing at least one high momentum, high transverse-momentum electron or muon accompanied by jets. The charge of one of the b-quarks is measured by the charge of its decay lepton. The charge of the other decaying b-quark is extracted from the momentum-weighted average charge of the jet fragments in the thrust hemisphere opposite to that of the lepton. The mixing parameters are then determined by comparing the lepton charge to the jet charge.

This method has the advantage, compared to the traditional dilepton approach, of a ten-fold increase in event statistics. Its systematic errors are mostly independent of those affecting the dilepton result. As the lepton charge and the jet charge are sensitive in different ways to B_d and B_s mixing, the result, expressed as a contour in the χ_d - χ_s plane, exhibits a slope different from that of the dilepton band. The combination of the two methods therefore has the potential to constrain the allowed range of B_s mixing. On the other hand, the jet charge is related to the quark charge in a statistical sense only; this leads to a dilution of the gain brought about by the increase in event sample size. In addition, the interpretation of the measurement relies on detailed Monte Carlo simulations of jet-charge distributions, which are sensitive to assumptions about the fragmentation and decay in heavy quark jets.

This paper is organised as follows. Section 2 establishes the principle of the method. After a brief sketch of the ALEPH detector and of the event selection procedure in Section 3, Section 4 describes how to extract the average b lepton-signed hemisphere charge from the data. This quantity is then interpreted in terms of mixing in Section 5. The errors are discussed in Section 6, and Section 7 deals with the combination of the jet-charge mixing measurement with the previously published ALEPH dilepton result. A summary is presented in Section 8.

[2]Throughout this paper, reference to a given charge state implies the charge-conjugate state, unless otherwise stated.

2 Principle of the Measurement

The discussion of this section assumes a pure sample of $Z \to b\bar{b}$ events containing a lepton from a primary semileptonic b decay. The lepton charge unambiguously tags the charge of the b quark in the decaying hadron. If this quark was contained in a baryon, a charged B meson or a neutral B meson that did not mix, then the charge has the same sign as that of the originally produced quark. If, on the other hand, a B^0 meson has undergone the transition into its antiparticle state $\bar{B}^0$ by flavour oscillations, the charge sign of its decay lepton is opposite to that of the quark produced in the original Z decay.

The charge of the other b quark in the event is inferred from its charged jet fragments, exploiting the correlation between the charges of high momentum particles in the jet and that of the parent quark. The same procedure is followed here as in the study of the hadronic charge asymmetry [5]. The plane perpendicular to the thrust axis separates the event into two hemispheres. In the hemisphere *opposite* to the lepton, the hemisphere charge

$$Q_H = \frac{\sum_i |\vec{p}_i \cdot \vec{e}_T|^\kappa \cdot q_i}{\sum_i |\vec{p}_i \cdot \vec{e}_T|^\kappa} \tag{2}$$

is defined as the momentum-weighted charge average over all charged particles in that hemisphere. $|\vec{p}_i \cdot \vec{e}_T|$ is the momentum component of particle i along the thrust axis, q_i is its charge, and κ is a weighting parameter chosen to optimise the sensitivity of the measurement. This analysis adopts $\kappa = 1$; the justification of this choice is deferred to section 6.

The lepton charge q_ℓ and the opposite-hemisphere charge Q_H together contain the information about mixing in the event. It is thus convenient to define the lepton-signed hemisphere charge,

$$Q_{\ell H} = -q_\ell \cdot Q_H \,,$$

such that it is positive if the hemisphere charge correctly reflects the charge sign of the original quark and the lepton originates from a b hadron that did not mix. The average lepton-signed hemisphere charge for b events with a primary lepton, $\langle Q_{\ell H} \rangle_b$, is the measured quantity that will be interpreted in terms of mixing. Since mixing reverses the sign of the lepton, it is related to χ by

$$\langle Q_{\ell H} \rangle_b = (1-\chi)\langle Q_{bH} \rangle + \chi \langle -Q_{bH} \rangle = (1-2\chi)\langle Q_{bH} \rangle \,, \tag{3}$$

Here, $\langle Q_{bH} \rangle$ is the average b quark-signed hemisphere charge, defined by

$$Q_{bH} = \text{sign}(q_b) \cdot Q_H,$$

where q_b is the charge of the b or $\bar{b}$ quark going into the *same* hemisphere as that in which the charge is reconstructed. This quantity is positive if the hemisphere charge correctly reflects the charge sign of the original quark in that hemisphere.

A detailed Monte Carlo study shows that the hemisphere charge retains information about the quark charge even when the b hadron is neutral. This can

be appreciated from Figs. 1a-c which show the momentum spectra, in the meson rest frame, of the long-lived charged particles originating from the expected mix of $B_d = (\bar{b}d)$ and $B_s = (\bar{b}s)$ decays. The positively charged particles exhibit a harder momentum spectrum than the negatively charged fragments. This asymmetry is most pronounced in the case of primary semileptonic decays (a), where a large momentum is transferred to a single positively charged particle. But it is also manifest in two-body (b) and in multi-body hadronic B meson decays (c) and is thus a general feature of the weak decay cascade.

Consequently, the momentum-weighted charge sum of B^0 decay products is positive. The hemisphere charge receives in addition the contribution from the fragmentation companions, which in a naive picture is related to the positive charge of a $\bar{d}$ quark, left over from the $d\bar{d}$ pair that was created to form a B_d meson (and similarly for B_s). The Monte Carlo study shows that the magnitudes of the two components are comparable. In the case where the B^0 meson has mixed, however, these two contributions cancel each other to a large extent. Therefore the average quark-signed hemisphere charge $\langle Q_{bH} \rangle$ depends itself on the mixing rates, as is clear in the decomposition:

$$\begin{aligned} \langle Q_{bH} \rangle &= (1 - f_d - f_s)\langle Q_{B_u} \rangle \\ &+ f_d(1 - \chi_d)\langle Q_{B_d} \rangle + f_d \cdot \chi_d \langle \bar{Q}_{B_d} \rangle \\ &+ f_s(1 - \chi_s)\langle Q_{B_s} \rangle + f_s \cdot \chi_s \langle \bar{Q}_{B_s} \rangle \ , \end{aligned} \tag{4}$$

where $\langle \bar{Q}_{B_q} \rangle$ and $\langle Q_{B_q} \rangle$ denote the average quark-signed charges for hemispheres containing B_q mesons ($q = d$, s) that did or did not mix, respectively. The first term includes all non-B^0 hadrons. f_d and f_s are the fractions of produced B_d and B_s mesons, respectively, in the pure b sample, and χ_q are the respective probabilities for mixing to occur:

$$\chi_q \equiv \frac{\Gamma(B_q^0 \to \bar{B}_q^0)}{\Gamma(B_q^0 \to B_q^0) + \Gamma(B_q^0 \to \bar{B}_q^0)} \ .$$

Inserting the full expression (4) into equation (3) yields a form quadratic in χ_d and χ_s: the sensitivity to mixing in the hemisphere *opposite* to the lepton actually contributes to the statistical sensitivity of this measurement.

The analysis is structured as follows. An event sample highly enriched in primary semileptonic b decays is selected among the Z events. The average b lepton-signed hemisphere charge $\langle Q_{\ell H} \rangle_b$ is extracted from these data. The average quark-signed charges $\langle Q_{B_u} \rangle$,..., $\langle \bar{Q}_{B_s} \rangle$ are obtained from a Monte Carlo calculation. The combination of Eqs. (3) and (4) is then used to derive a constraint on the mixing parameters χ_d and χ_s from the measurement.

3 ALEPH Detector and Event Selection

Only a sketch of the ALEPH detector is presented here, as it has been described in detail elsewhere [6]. Charged particle momenta are measured by an inner cylindrical drift chamber (ITC) and by a large cylindrical time projection chamber (TPC)

that surrounds it. These are immersed in a 1.5 T magnetic field. The TPC also measures the specific ionisation of each charged track. A finely segmented, lead-proportional-tube electromagnetic calorimeter (ECAL) is placed between the TPC and the superconducting coil. Outside the coil lies the hadron calorimeter (HCAL): it consists of iron slabs interleaved with layers of limited-streamer tubes, and combines the functions of magnetic return yoke, hadron calorimeter, and muon filter. Finally, the detector is enclosed by two additional outside layers of streamer tubes, that provide 3-dimensional track points and complement the muon identification role of the HCAL.

The event selection criteria are essentially identical to those applied in the study of the $b\bar{b}$ forward-backward asymmetry [7]. Briefly, hadronic Z decays are first selected by requiring the event to contain at least 5 validated charged tracks, that together carry at least 10% of the centre-of-mass energy. In addition, the thrust axis (determined from both charged and neutral particles) must lie within a polar angle window defined by $|\cos\theta| < 0.85$. The resulting sample is then enriched in $Z \rightarrow b\bar{b}$ decays by requiring in addition the presence of at least 2 jets, and at least one high momentum electron or muon. Jets are formed with a scaled-invariant-mass clustering algorithm, using all charged tracks and electromagnetic and hadronic energy clusters not associated to tracks. Electrons are identified by matching a charged track measured in the TPC and ITC with an energy deposition in the ECAL that is consistent in specific ionisation, shower energy and shower profile with those of an electron of the measured momentum. Muon identification is achieved by the association of a charged track with a pattern of hits in the HCAL and the muon chambers consistent with the muon hypothesis. The same methods as those presented in refs. [4, 8] are used to remove photon conversions and Dalitz pairs from the prompt electron signal, and to estimate from the data the lepton identification efficiency and the background to the electron and muon samples.

The final sample is based on the analysis of approximately 180,000 hadronic Z decays collected in 1989 and 1990. It consists of the hadronic events containing at least two jets, and at least one lepton candidate that satisfies $p \geq 3.0\,\mathrm{GeV}$ and $p_\perp \geq 0.5\,\mathrm{GeV}$, where the lepton transverse momentum $p_\perp$ is defined with respect to the jet axis calculated with the lepton included. About 69% of the 11,147 leptons in this heavy-flavour enhanced sample originate from b decays, the remainder being due to semileptonic decays of primary charm, non-prompt leptons (unidentified conversions or Dalitz pairs or muon decays in flight), and hadrons misidentified as electrons or muons. Maximum-likelihood fits to the electron and muon p, $p_\perp$ spectra, similar to those described in ref. [7], are used to assign to each lepton a set of probabilities for it to originate from one of the processes listed in Table 1. These probabilities $\mathcal{P}_{pb}...\mathcal{P}_{bg}$, depend on the lepton flavour (e or μ) and on its p and $p_\perp$. Averaging the subprocess probabilities over all leptons in the sample yields the fractional flavour composition listed in the table.

Process	label		%
$b \to \ell$			
$b \to \tau \to \ell$	}	pb	54
$b \to W \to \bar{c} \to \ell$			
$b \to c \to \ell$		bc	15
$c \to \ell$			13
non − prompt leptons	}	bg	12
misidentified hadrons			6

Table 1: *Flavour composition of the inclusive lepton sample.*

4 Determination of the average b lepton-signed hemisphere charge

The measured lepton-signed hemisphere charge, averaged over the N_ℓ leptons in the sample, receives contributions from all the subprocesses listed above:

$$\langle Q_{\ell H}^{meas} \rangle = \frac{1}{N_\ell} \sum_l (\mathcal{P}_{pb} - \mathcal{P}_{bc})_l \langle Q_{\ell H} \rangle_b + \frac{1}{N_\ell} \sum_l (\sum_{bg} \mathcal{P}_{bg} \langle Q_{\ell H} \rangle_{bg})_l \qquad (5)$$

where l runs over all leptons. The first term, $\langle Q_{\ell H} \rangle_b$, on the right-hand side of this equation carries the mixing information, as discussed in Sec. 2. As the cascade process flips the sign of the decay lepton, the lepton-signed hemisphere charges for primary ($b \to l$) and cascade ($b \to c \to l$) decays are equal in magnitude but opposite in sign[3]: $\langle Q_{\ell H} \rangle_b = \langle Q_{\ell H} \rangle_{pb} = -\langle Q_{\ell H} \rangle_{bc}$.

The second term in Eq. (5) describes the background component of the measured hemisphere charge:

$$\begin{aligned} \sum_{bg} \mathcal{P}_{bg} \langle Q_{\ell H} \rangle_{bg} &= \mathcal{P}_{pc} \cdot \langle Q_{\ell H} \rangle_{pc} \\ &+ \mathcal{P}_{np} \cdot \langle Q_{\ell H}(p, p_\perp, \text{ e or } \mu) \rangle_{np} \\ &+ \mathcal{P}_{mh} \cdot \langle Q_{\ell H}(p, p_\perp, \text{ e or } \mu) \rangle_{mh} \end{aligned} \qquad (6)$$

The mean charm hemisphere charge $\langle Q_{\ell H} \rangle_{pc}$ must be obtained by Monte Carlo simulation, whilst those of non-prompt leptons (np) and misidentified hadrons (mh) are extracted from the data themselves. To this effect, samples of "fake electrons" and "fake muons" are selected. These satisfy the same selection criteria as the genuine electron or muon candidates, except that the fake lepton track must be unambiguously identified as a hadron. The average fake-lepton signed hemisphere charge can then be computed directly from that data sample and tabulated as a function of the p and $p_\perp$ of the track.

[3]The mixing parameter χ, as defined in Eq. (1), extracted from a pure sample of $b \to c \to l$ decays, would differ by a few percent from that extracted from primary $b \to l$ decays, because the semileptonic branching ratios of charged and neutral charm mesons are not equal. The cascade decays are sufficiently suppressed in this analysis by the (p, $p_\perp$) cuts on the lepton for this effect to be negligible.

Figure 2 compares the measured distribution of lepton-signed hemisphere charges with the sum of the contributions expected from the various flavour subprocesses. The shapes of the charge distributions expected from b- and c-produced leptons are extracted from a Monte Carlo simulation that incorporates the level of B^0-$\bar{B}^0$ mixing previously measured by the dilepton method [4]. Contributions from non-prompt leptons and misidentified hadrons model the shape of the fake-lepton-signed charge distributions as a function of the p and $p_\perp$ of the track. The overall agreement between the predicted and observed $Q_{\ell H}^{meas}$ distributions is acceptable[4].

In principle the average b lepton-signed hemisphere charge can be extracted by simply combining equations (5) and (6) and solving for $\langle Q_{\ell H}\rangle_b$. However, this procedure ignores the fact that higher-$p_\perp$ leptons, for instance, are much more likely to originate from b- than from c-decay. In order to maximise the use of available information, a weighted mean method is applied:

$$\langle Q_{\ell H}\rangle_b = \frac{\sum_l W_l \cdot (Q_{\ell H}^{meas} - \sum_{bg} \mathcal{P}_{bg}\langle Q_{\ell H}\rangle_{bg})_l}{\sum_l W_l \cdot (\mathcal{P}_{pb} - \mathcal{P}_{bc})_l}$$

where $W_l(P, P_\perp)$ is a weighting factor reflecting the probability of lepton l to have originated from b semileptonic decay. It can be shown that using $W_l = \mathcal{P}_{pb} - \mathcal{P}_{bc}$ optimises the statistical sensitivity of the method. This finally gives

$$\langle Q_{\ell H}\rangle_b = 0.0863 \pm 0.0069\,(\text{stat.})\,.$$

This measurement is affected by systematic errors arising from uncertainties in the flavour composition of the inclusive lepton sample, and in the Monte Carlo modelling of the quark-signed hemisphere charge for c quarks (the error due to event selection and detector systematics was found to be negligible). To study the magnitude of the flavour composition error, the relative fractions of primary b-decays, cascade $b \to c \to l$ decays, primary c decays, non-prompt leptons, and misidentified hadrons, are varied to the same extent as in ref. [7]. This results in a total error due to flavour composition of $\pm$ 0.0017 on $\langle Q_{\ell H}\rangle_b$ (a detailed breakdown is presented in the Appendix). The uncertainty on the average quark-signed hemisphere charge for charm events is estimated by varying a number of parameters (listed in the Appendix) in the Monte Carlo model, which affect the hadronisation and decay of charm jets. The resulting uncertainty on the charm background subtraction leads to an error of $\pm$ 0.0006 on $\langle Q_{\ell H}\rangle_b$.

Combining the above results yields for the measured lepton-signed hemisphere charge in b events (at $\kappa = 1$) :

$$\langle Q_{\ell H}\rangle_b = 0.0863 \pm 0.0069\,(\text{stat.}) \pm 0.0018\,(\text{syst.})\,. \qquad (7)$$

[4]A quantitative comparison yields $\chi^2 = 93$ for 48 degrees of freedom. As the largest discrepancy occurs in the limited range $-0.85 < Q_{\ell H}^{meas} < -0.65$, the analysis was repeated with stringent cuts on the absolute value of the hemisphere charge, excluding that region from the data. The stability of the final result when varying this cut lies well within the systematic error quoted in Sec. 6.

5 Interpretation of $\langle Q_{\ell H} \rangle_b$ in terms of mixing

Interpreting the above measurement in terms of mixing requires the *a priori* knowledge of the average quark-signed hemisphere charges for b hadrons, $\langle Q_{B_u} \rangle$,..., $\langle \bar{Q}_{B_s} \rangle$ (Eq. (4)). These are extracted from a detailed Monte Carlo simulation of $Z \to b\bar{b}$ events as reconstructed in the ALEPH detector. Events are generated using the DYMU package [9]. This generator is interfaced to the Lund string model with parton shower evolution [10] and updated decay tables for the charm and beauty hadrons.

With that input, Eq. (3) translates the measurement of $\langle Q_{\ell H} \rangle_b$, with its error, into a constraint on the mixing parameters, that can be represented by a 68% confidence level contour in the χ_d-χ_s plane (Fig. 3a). Since a line of constant $\langle Q_{\ell H} \rangle_b$ exhibits negligible curvature (its slope varies by 2% of itself over the full χ_s range), the result (7) can be expressed to a very good approximation as

$$f_d \chi_d = (0.113\ ^{+0.033}_{-0.032}) - (0.72 \pm 0.03) f_s \chi_s \,. \tag{8}$$

The error, which is reflected in the width of the band in Fig. 3a, combines all the statistical and systematic uncertainties that will be discussed in the following section.

For comparison, the ALEPH mixing measurement based on dileptons [4]

$$\chi \;=\; f_d \chi_d \;+\; f_s \chi_s \;=\; 0.132^{+0.027}_{-0.026} \tag{9}$$

results in a similar band (Fig. 3b), but with a slope that is steeper than that of the jet-charge result. This arises for the following reason. After introducing

$$\begin{aligned} \langle Q_{bH} \rangle^{\chi=0} &= (1 - f_d - f_s)\langle Q_{B_u} \rangle + f_d \langle Q_{B_d} \rangle + f_s \langle Q_{B_s} \rangle \,, \\ \Delta_{Q_d} &= 1/2 \cdot (\langle Q_{B_d} \rangle - \langle \bar{Q}_{B_d} \rangle) \,/\, \langle Q_{bH} \rangle^{\chi=0} \,, \\ \Delta_{Q_s} &= 1/2 \cdot (\langle Q_{B_s} \rangle - \langle \bar{Q}_{B_s} \rangle) \,/\, \langle Q_{bH} \rangle^{\chi=0} \,, \end{aligned} \tag{10}$$

the combination of Eqs. (3) and (4) can be rewritten as

$$\frac{\langle Q_{\ell H} \rangle_b}{\langle Q_{bH} \rangle^{\chi=0}} = (1 - 2\chi)(1 - 2(f_d \chi_d \Delta_{Q_d} + f_s \chi_s \Delta_{Q_s})) \,. \tag{11}$$

This form[5] exhibits the parallel between the lepton- and the hemisphere-charge terms. But it also shows that while leptonic decays provide equal sensitivity to mixing in B_d and B_s events, the b hemisphere charge depends on the normalised sensitivities Δ_{Q_d} and Δ_{Q_s} (Eq. (10)), which are not equal. This is due to the fact that the predominant decay chains for the two species are expected to be distinct:

$$\begin{aligned} B_d &\longrightarrow D^{*-} X \\ &\qquad \hookrightarrow \bar{D}^0 \pi^- \,, \\ B_s &\longrightarrow D_s^{*-} X \\ &\qquad \hookrightarrow D_s^- \gamma. \end{aligned}$$

[5] Eqs. (9) and (11) assume that the semileptonic branching ratios of B_d and B_s mesons are equal to the average b hadron semileptonic branching ratio.

In the first case, the soft pion contributes little to the momentum-weighted hemisphere charge, and even sometimes escapes detection altogether. As the charge it carries (opposite in sign to that of the $\bar{b}$ quark) is, in this sense, "missing", the contribution to the hemisphere charge of the other B_d decay products is enhanced. The B_s decay chain involves a photon rather than a pion: in this case there is no such charge enhancement. Therefore $\Delta_{Q_d} > \Delta_{Q_s}$, so that the b quark-signed hemisphere charge is more sensitive to B_d mixing than it is to B_s mixing.

6 Error Analysis

Three components contribute to the total error affecting the jet-charge analysis:

- the statistical accuracy on the measured b lepton-signed hemisphere charge $\langle Q_{\ell H} \rangle_b$,
- the systematic error on $\langle Q_{\ell H} \rangle_b$,
- systematic uncertainties in the modelling of the b quark-signed hemisphere charges required to interpret $\langle Q_{\ell H} \rangle_b$ in terms of mixing, including the dependence of the final result on the choice of the momentum weighting power κ (Eq. (2)).

The statistical and systematic errors affecting $\langle Q_{\ell H} \rangle_b$ have been addressed in Sec. 4. Besides the mere size of the event sample, the statistical error reflects the width of the hemisphere charge distribution and the dilution caused by cascade decays. Although these decays only constitute 22% of the b signal (Table 1), they increase the statistical error affecting the measurement of the mixing rate by about 40%. The systematic error, in turn, arises from uncertainties in the flavour composition of the sample and the average charm jet charge, which affect the background subtraction. In the χ_d-χ_s plane all these errors correspond to a translation of the line of constant $\langle Q_{\ell H} \rangle_b$ parallel to itself.

The third error above, which dominates the systematic uncertainty, reflects the imperfect knowledge of the heavy quark fragmentation and decay properties that influence the calculation of the average b quark-signed hemisphere charges. This error is estimated by varying separately each one of 13 Monte Carlo parameters (listed in the Appendix) over ranges justified in Refs. [5, 11]. Repeating the analysis with the new values of the b hemisphere charges corresponding to each parameter setting, results in translations of the line of constant $\langle Q_{\ell H} \rangle_b$ almost parallel to itself. The slope of that line changes by amounts small compared to the error on its $\chi_s = 0$ intercept.

To allow direct comparison with the errors of dilepton experiments, it is convenient to express the width of the error band in terms of a single quantity stated in the same units as the dilepton mixing parameter χ. This can be visualised as the intersection of the jet-charge confidence band (Fig. 3a) with the χ_d axis, and is equivalent to the error on the mixing parameter χ for any fixed value of χ_s:

$$\Delta\chi|_{\chi_s=\text{const.}} = f_d \cdot \Delta\chi_d \quad . \tag{12}$$

Table 2 lists the main contributions to the total systematic error; a more detailed breakdown is presented in the Appendix. The b fragmentation function and branching ratios provide the largest known sources of systematic error.

Error source	$\Delta\chi\|_{\chi_s=\text{const.}}$	
$\langle Q_{\ell H}\rangle_b$ (stat.)	+0.018	-0.018
$\langle Q_{\ell H}\rangle_b$ (syst., flavour composition)	+0.004	-0.004
Fragmentation and decay model	+0.016	-0.020
Monte Carlo statistics	+0.003	-0.003
Combined stat. + syst. (at $\kappa = 1$)	+0.024	-0.027
κ-dependence	+0.022	-0.016
Total error	+0.033	-0.032

Table 2: *Contributions to the error, $\Delta\chi|_{\chi_s=\text{const.}}$, affecting the mixing measurement by the jet-charge method. Statistical and systematic errors at $\kappa = 1$ are combined in quadrature; the resulting subtotal and the κ-dependence error, again added in quadrature, yield the total error.*

The stability of the final result with respect to the momentum-weighting power κ (Eq. (2)) provides an independent check of the systematic error estimate. An *a priori* choice of κ between 0.5 and 1 optimises simultaneously the average charge tagging efficiency in b jets, and the sensitivity of the b hemisphere charge to mixing. This is first illustrated in Fig. 4a which displays, as a function of κ, the charge separation power S_{charge}, defined as the ratio of the mean and width of the b quark-signed hemisphere charge distribution:

$$S_{\text{charge}} = \langle Q_{bH}\rangle / \sigma_{Q_{bH}}$$

This is maximal near $\kappa = 0.5$, and decreases for large weighting powers, where only information from the fastest particles is used. Next, the sensitivity of the quark-signed hemisphere charge itself to mixing, S_{mix}, can be expressed as the difference between the average charges of hemispheres containing B^0 mesons that did not or did mix, normalised to the width of the distribution:

$$S_{\text{mix}} = (\langle Q_{bH}\rangle^{\text{not mixed}} - \langle Q_{bH}\rangle^{\text{mixed}}) / \sigma^{\text{not mixed}}_{Q_{bH}} .$$

S_{mix} increases with increasing κ until reaching a plateau around $\kappa = 1$ (Fig. 4b).

A posteriori, the above criteria are confirmed by the κ-dependence of the statistical error on the mixing measurement (Fig. 4c), which exhibits a minimum around $\kappa = 0.7$. On the other hand, the systematic error, shown in the same figure, increases towards low κ values, where the predicted b charges become more sensitive to details of the soft hadronisation mechanism. The resulting overall minimum of the combined statistical and systematic errors justifies the choice of $\kappa = 1$.

Table 3 lists the variation $\delta\chi|_{\chi_s=\text{const.}}$ of the jet-charge result, compared to its value at $\kappa = 1$, for a few κ values around the optimum. As these measurements are based on the same data sample, their correlation must be taken into account when evaluating the statistical significance of the difference. The table indicates that part,

κ	$\delta\chi\|_{\chi_\kappa=\text{const.}}$		
0.3	-0.033	$\pm$	0.011
0.5	-0.016	$\pm$	0.007
1.0	0.0	$\pm$	0.0
2.0	+0.022	$\pm$	0.006

Table 3: *κ-dependence of the jet-charge mixing result. The table lists the change relative to $\kappa = 1.0$, and the one-standard-deviation statistical error on that change, taking into account the correlations between the lepton-signed jet charges measured at different κ values.*

but not all, of the observed dependence on κ may be due to statistical fluctuations between the high- and low-momentum ends of the charged particle spectrum.

By a suitable choice of some of the parameters controlling the Monte Carlo event simulation, it is possible to substantially reduce this discrepancy, but it could not be eliminated completely. This suggests that the fragmentation and decay model used does not describe the details of the charged particle spectrum in $b\bar{b}$ events with sufficient accuracy. The systematic error on this measurement is therefore increased by an additional uncertainty corresponding to the full observed variation of the result over the range $0.5 < \kappa < 2$. This procedure conservatively includes in the systematic error a possible contribution of statistical fluctuations, as well as part of the systematic error already associated to the fragmentation model. The total error thus obtained is given in Table 2 and displayed in Fig. 3a.

7 Combination of the dilepton and jet-charge mixing measurements

The mixing measurement derived from the jet-charge analysis, shown in Fig. 3a, can now be combined with the previously published ALEPH dilepton result based on the same data sample, $\chi = 0.132 \pm 0.022 \pm 0.014$ (Fig. 3b) [4]. In doing so, however, the small correlation between the two methods must be taken into account.

First, there exists a small statistical correlation as the dilepton events are included in the jet-charge analysis. This is done in order to avoid an additional systematic error due to the dependence of the b hemisphere charge parametrisation itself on the momentum cut used in the dilepton selection. The dilepton events, as selected in Ref. [4], amount to 8% of the event sample used in the jet-charge analysis, and hence represent 16% of the inclusive lepton count. To take this into account the statistical error affecting the jet-charge result (Eq. (7)) is inflated (for combination purposes only) by a factor of 1.14, evaluated by explicitly excluding the dilepton events from the analyzed sample.

The systematic errors are very different in the two methods. The jet-charge analysis suffers mostly (Table 2) from uncertainties in the modelling of the b hemisphere charge distributions, while the error due to the lepton fractions represents a small contribution. In contrast, the dilepton systematic error [4] is dominated

by flavour composition uncertainties. This is a consequence of the fact that the fractions of leptons from a given source enter only linearly into the evaluation of $\langle Q_{\ell H} \rangle_b$ (Eqs. (5), (6)), whereas the dilepton result depends on products of such fractions. The full correlated flavour-composition error is taken into account by removing its contributions from the individual dilepton and jet-charge errors, and adding in quadrature, to the combined total error, a weighted linear sum of these two individual error contributions.

The results of mixing measurements using either the dilepton method or the jet-charge technique can be expressed independently of assumptions on the production fractions f_d and f_s (Eqs. (8) and (9)). However, because of the different sensitivities of the two methods to the B_d and B_s mixing rates, the combined result depends in principle on these fractions. In practice the corresponding error is negligible.

The combined 68% confidence level contour in the $\chi_d - \chi_s$ plane, with the above considerations taken into account, summarises the ALEPH measurement of B^0-$\bar{B}^0$ mixing. It is shown in Fig. 5, together with the ARGUS and CLEO measurement of $\chi_d = 0.167 \pm 0.042$ [1] and with the Standard Model prediction [13]. The axis of the band is no longer quite parallel to the dilepton contour described by χ = constant. At the present level of accuracy, however, it is convenient to project this two-dimensional contour onto an axis measuring χ. Strictly speaking, this corresponds to quoting a value corresponding to χ_s fixed in the middle of its physical range. The bias introduced by the projection is small, ± 0.003, and is included in the total error. At the cost of a slight loss of information, the combined ALEPH mixing result can thus be expressed as a single number:

$$\chi = 0.129 \pm 0.022 \ .$$

where the error quoted combines all statistical and systematic uncertainties[6].

8 Summary

B^0-$\bar{B}^0$ mixing in e^+e^- annihilation has been measured by a jet-charge method, using a sample enriched in $Z \rightarrow b\bar{b}$ decays by a high momentum, high transverse momentum inclusive single lepton tag. The mixing information is extracted from the comparison of the lepton charge to the momentum-weighted average charge in the thrust hemisphere opposite to the lepton. The fundamental quantity measured is the b lepton-signed hemisphere charge:

$$\langle Q_{\ell H} \rangle_b = 0.0863 \pm 0.0069 \pm 0.0018,$$

where the first error is statistical, and the second systematic.

This result translates into a 68% confidence level contour in the $\chi_d - \chi_s$ plane, parametrised as

$$f_d \chi_d + 0.72 f_s \chi_s = 0.113 \pm 0.018 \pm 0.027 \ .$$

[6]Note that the correlations discussed in this section have little impact on the result: combining the dilepton and jet-charge measurements under the assumption that they are completely independent would yield $\chi = 0.128 \pm 0.020$.

Combining it with the previously published ALEPH dilepton measurement, $\chi = f_d\chi_d + f_s\chi_s = 0.132 \pm 0.022 \pm 0.014$, defines an improved contour in the mixing plane which, if described in terms of the dilepton mixing parameter, yields

$$\chi = 0.129 \pm 0.022 \ .$$

Acknowledgements

We thank our colleagues of the SL division for the good performance of the LEP accelerator. Thanks are also due to the engineering and technical personnel at CERN and at the home institutes for their contributions to the success of ALEPH. Those of us not from member states wish to thank CERN for its hospitality.

Appendix: Systematic Errors

This appendix contains a detailed breakdown of the systematic errors affecting the measurement of mixing by the jet-charge method.

Table 4 details the flavour composition uncertainties affecting the b lepton-signed hemisphere charge, as discussed in Sec. 4. The central values and the errors assumed for the semileptonic branching ratios are discussed in Ref. [7]. The table lists, for each flavour subprocess, the relative uncertainty assigned to the corresponding lepton rate, the systematic error this uncertainty induces on $\langle Q_{\ell H}\rangle_b$, and the impact of this error on the jet-charge mixing result, expressed in terms of $\Delta\chi|_{\chi_s=\text{const.}}$ (Eq.(12)).

Process	Relative uncertainty	Systematic error $\Delta\langle Q_{\ell H}\rangle_b$		$\Delta\chi\|_{\chi_s=\text{const.}}$	
$b \to \ell$	$\pm$ 0.10	+0.0013	-0.0013	+0.003	-0.003
$b \to c \to \ell$	$\pm$ 0.10	+0.0009	-0.0010	+0.003	-0.002
$b \to W \to \bar{c} \to \ell$	$\pm$ 0.50	+0.0001	-0.0003	+0.001	-0.000
$c \to \ell$	$\pm$ 0.20	+0.0002	-0.0002	+0.001	-0.001
non-prompt leptons (e/μ)	$\pm$ 0.2/0.1	+0.0005	-0.0004	+0.001	-0.001
misidentified hadrons (e/μ)	$\pm$ 0.2/0.4	+0.0004	-0.0003	+0.001	-0.001
Total, flavour composition		+0.0017	-0.0017	+0.004	-0.004

Table 4: *Systematic errors on the measured lepton-signed b hemisphere charge due to uncertainties in the flavour composition of the lepton sample.*

The systematic uncertainty on the interpretation of $\langle Q_{\ell H}\rangle_b$ in terms of mixing stems from the dependence of the calculated b quark-signed hemisphere charges on the fragmentation and decay parameters in the Monte Carlo simulation. Table 5 shows the impact on the jet charge mixing result of varying the 13 most important parameters. For each quantity, the table lists the central value adopted for the modelling of the charge distributions, the range over which it is varied, and the resulting systematic uncertainty $\Delta\chi|_{\chi_s=\text{const.}}$ (including the small error due to charm background subtraction). The ranges of variation are either based on measurements, or given by theoretical constraints. They are in most cases the same as in Ref. [5], and are justified in the Appendix of that publication. The table takes account of recent results on charmed meson production [12]. In addition, as some specific decay modes have a pronounced impact on the inclusive charged particle spectrum in B decays, it also includes conservative errors on the branching fractions [11] of semileptonic b decays and inclusive $B^0 \to D^{*-}X$ decays, and on the produced b baryon fraction.

Quantity	Central value	Range	Systematic error $\Delta\chi\|_{\chi_s=\text{const.}}$	
ϵ_b	0.006	0.003-0.010	+0.009	-0.012
ϵ_c	0.048	0.034-0.067	+0.001	-0.001
$(\frac{V}{V+PS})_{u,d}$	0.50	0.30-0.75	+0.004	-0.005
$(\frac{V}{V+PS})_s$	0.60	0.50-0.75	+0.000	-0.000
$(\frac{V}{V+PS})_{c,b}$	0.75	0.65-0.80	+0.002	-0.004
$\frac{s}{u}$	0.30	0.27-0.40	+0.002	-0.006
Λ_{QCD}	0.31	0.26-0.40	+0.001	-0.000
M_{min}	1.50	1.00-2.00	+0.000	-0.000
σ	0.36	0.34-0.40	+0.001	-0.000
b	0.84	0.75-0.93	+0.007	-0.008
$BR(b \to e, \text{or } \mu)$	0.103	0.093-0.113	+0.005	-0.005
$BR(B^0 \to D^{*-}X)\ BR(D^{*-} \to \bar{D}^0\pi^-)$	0.34	0.24-0.44	+0.006	-0.005
f_{baryon}	0.091	0.064-0.118	+0.006	-0.007
Total, fragmentation and decay model			+0.016	-0.020

Table 5: *Systematic errors* $\Delta\chi|_{\chi_s=\text{const.}}$ *due to uncertainties in parameters controlling the Monte Carlo simulation of b and c hemisphere charge distributions.*

References

[1] H. Albrecht *et al.* (Argus Collab.), Phys. Lett. B **192** (1987) 245.
M. Artuso *at al.* (CLEO Collab.), Phys. Rev. Lett. **62** (1989) 2b33.

[2] C. Albajar, *et al.* (UA1 Collab.), Phys. Lett. B **262** (1991) 171.

[3] H.R. Band *et al.* (MAC collab.), Phys. Lett. B **200** (1988) 221.
A. J. Weir *et al.* (Mark II Collab.), Phys. Lett. B **240** (1990) 289.
B. Adeva *et al.* (L3 Collab.), Phys. Lett. B **252** (1990) 703.
P.D. Acton *et al.* (OPAL Collab.), CERN-PPE-91-212 (1991).

[4] D. Decamp, *et al.* (ALEPH Collab.), Phys. Lett. B **258** (1991) 236.

[5] D. Decamp, *et al.* (ALEPH Collab.), Phys. Lett. B **259** (1991) 377.

[6] D. Decamp *et al.* (ALEPH Collab.), Nucl. Inst. and Meth. **A294** (1990) 121.

[7] D. Decamp, *et al.* (ALEPH Collab.), Phys. Lett. B **263** (1991) 325.

[8] D. Decamp, *et al.* (ALEPH Collab.), Phys. Lett. B **244** (1990) 551.

[9] J.E. Campagne and R. Zitoun, Z. Phys. C **43** (1989) 469.

[10] M. Bengtsson and T. Sjöstrand, Phys. Lett. B **185** (1987) 435.

[11] M. Aguilar-Benitez *et al.* (Particle Data Group) , Phys. Lett. B **239** (1990).

[12] D. Decamp, *et al.* (ALEPH Collab.), Phys. Lett. B **266** (1991) 218.

[13] P.J. Franzini, Phys. Rep. **173** (1989) 1.

Figure captions

Figure 1: Monte Carlo generated momentum spectra for positively (dots) and negatively (triangles) charged long-lived B^0 daughters (77% B_d and 23% B_s). The spectra are shown in the rest frame of the decaying meson, for (a) semi-leptonic decays, (b) two-body decays, and (c) multi-body decays.

Figure 2: Comparison of measured and predicted lepton-signed hemisphere charge distributions. The dots with errors bars represent the data. The histograms represent the predicted cumulative contributions of the flavour subprocesses listed in Table 1.

Figure 3: 68% confidence level contours, in the χ_d-χ_s plane, representing the ALEPH mixing measurements, using (a) the jet charge method and (b) the dilepton method. The figures are drawn assuming $f_d = 0.40$, $f_s = 0.12$.

Figure 4: κ-dependence of (a) the average charge separation power in b jets, S_{charge}, (b) the sensitivity of b jets to mixing, S_{mix}, and (c) the statistical (square), systematic (triangles) and total (circles) error in terms of $\Delta\chi|_{\chi_s=\mathrm{const.}}$.

Figure 5: 68% confidence level contour, in the χ_d-χ_s plane, representing the combined ALEPH jet charge and dilepton mixing measurement. Also shown are the combined result from ARGUS and CLEO [1], and the region allowed by the Standard Model [13]. The figure is drawn assuming $f_d = 0.40$, $f_s = 0.12$.

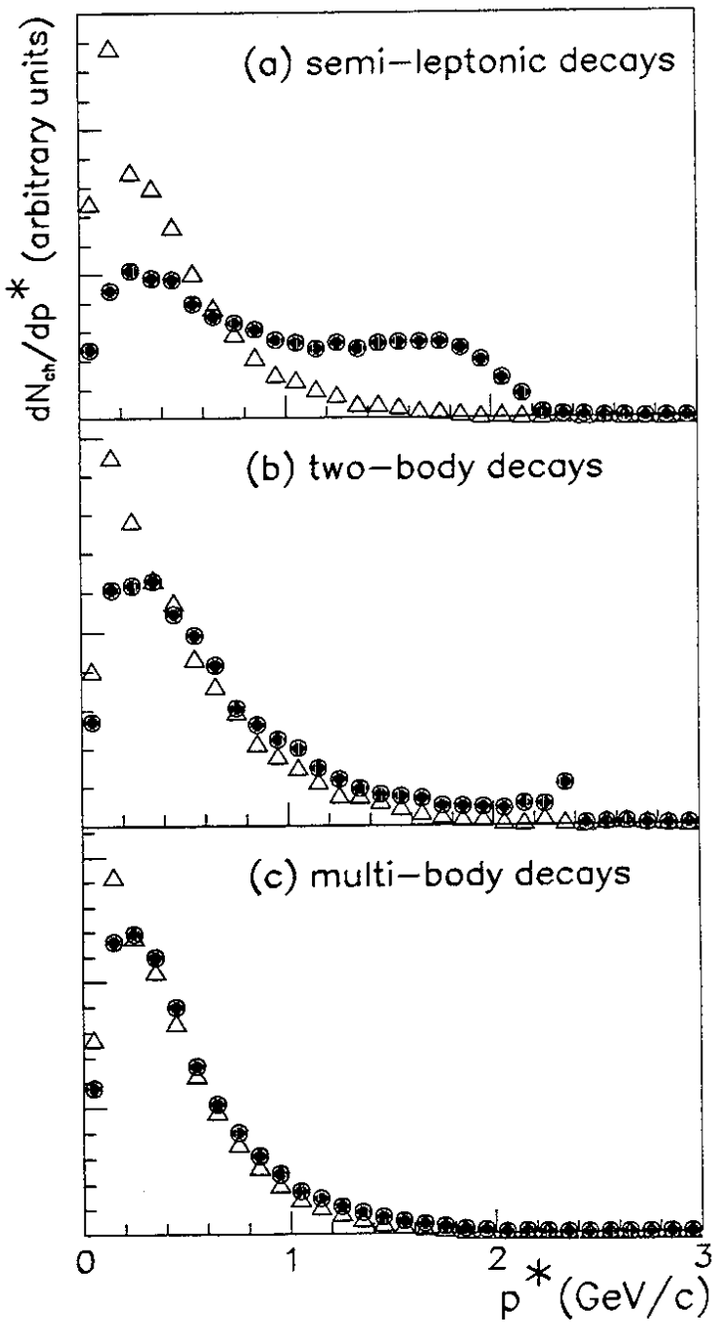
(a) semi−leptonic decays
(b) two−body decays
(c) multi−body decays
dN_{ch}/dp^* (arbitrary units)
0
1
2
3
p^* (GeV/c)

Figure 1

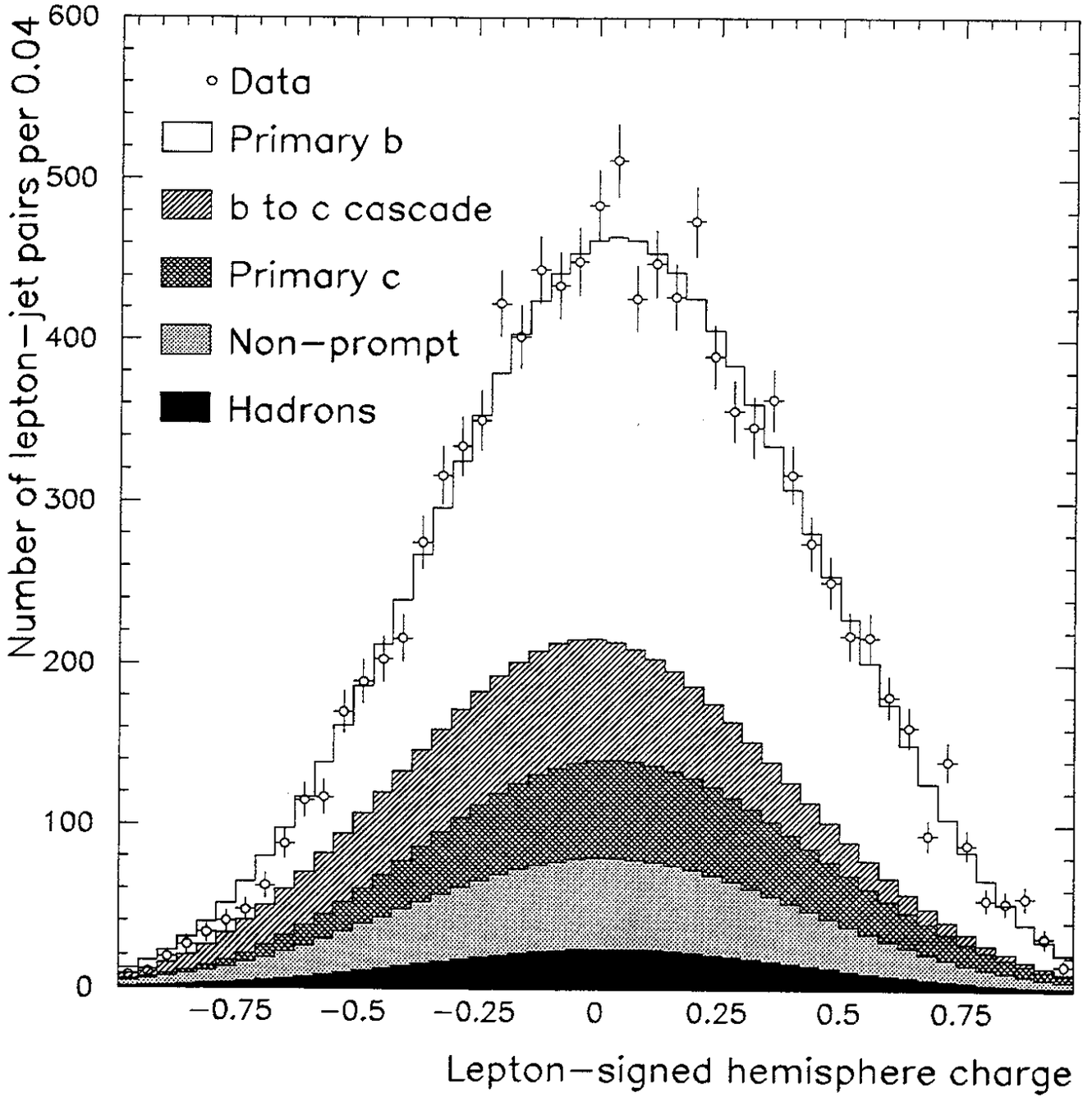
Data
Primary b
b to c cascade
Primary c
Non−prompt
Hadrons
Number of lepton−jet pairs per 0.04
600
500
400
300
200
100
0
−0.75
−0.5
−0.25
0
0.25
0.5
0.75
Lepton−signed hemisphere charge

Figure 2

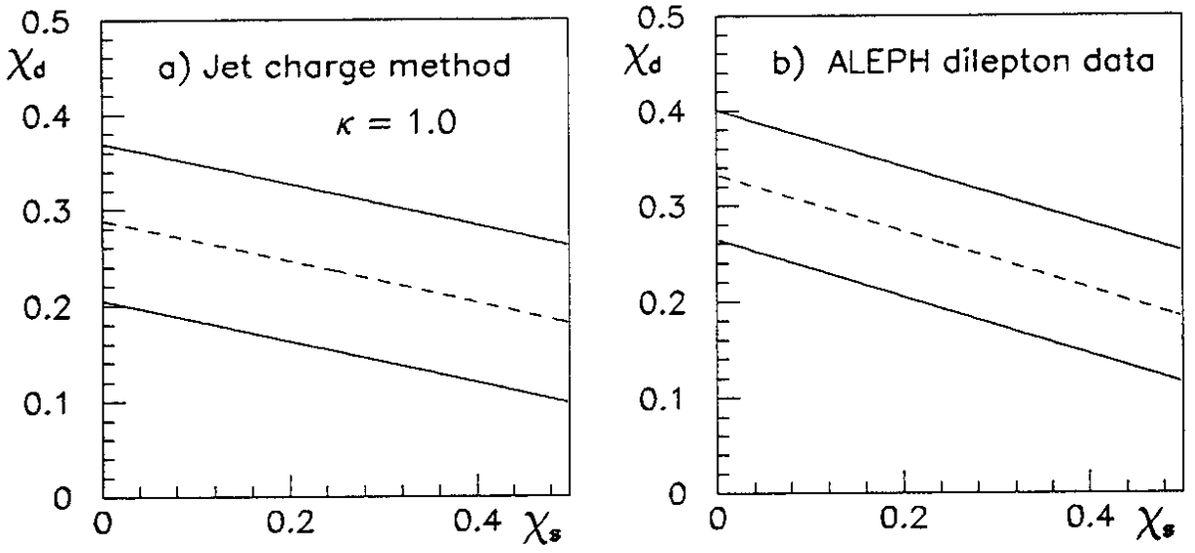
0.5
χ_d
0.4
0.3
0.2
0.1
0
a) Jet charge method
$\kappa = 1.0$
0
0.2
0.4
χ_s
0.5
χ_d
0.4
0.3
0.2
0.1
0
b) ALEPH dilepton data
0
0.2
0.4
χ_s

Figure 3

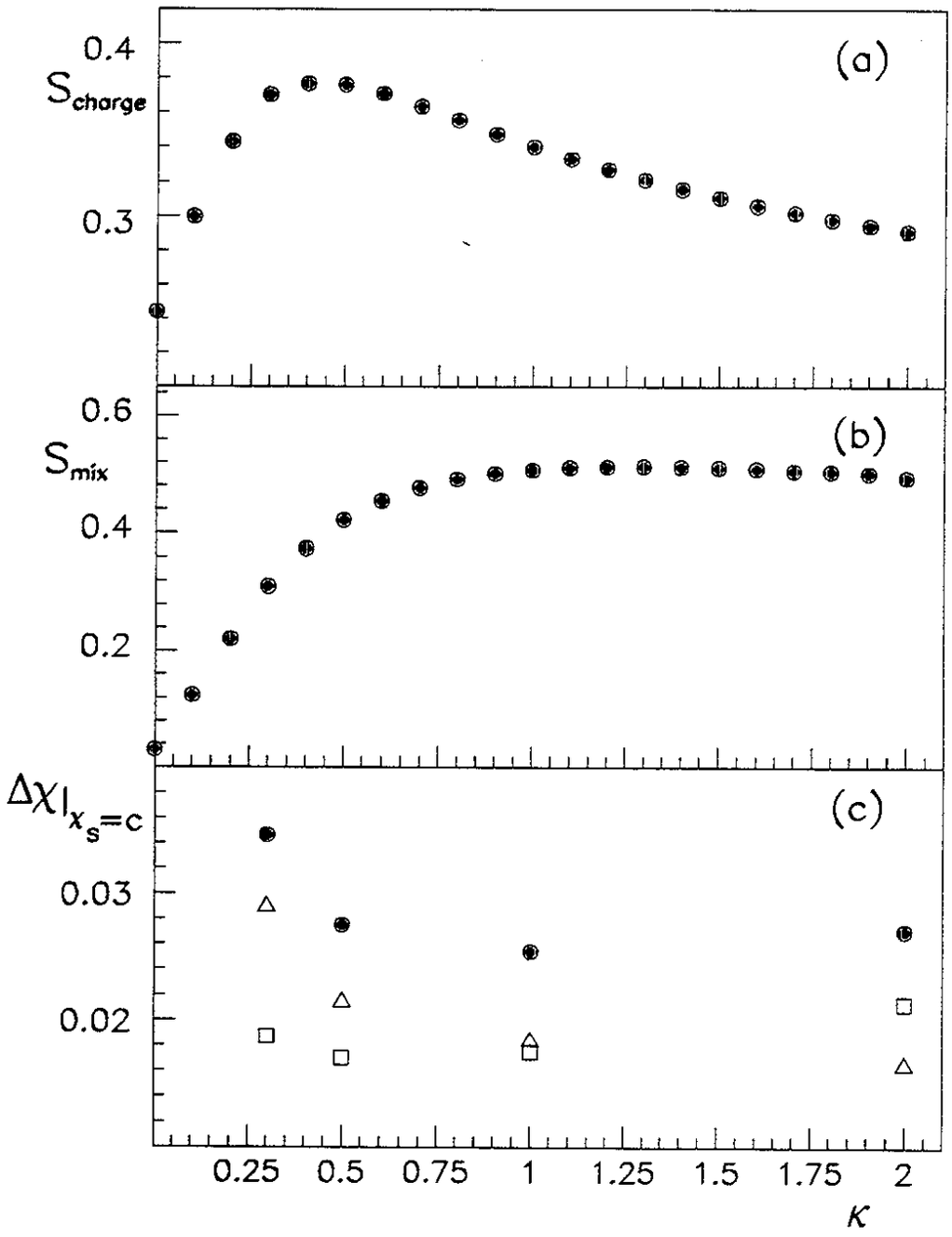
0.4
S_{charge}
0.3
(a)
0.6
S_{mix}
0.4
0.2
(b)
$\Delta\chi|_{x_s=c}$
0.03
0.02
(c)
0.25
0.5
0.75
1
1.25
1.5
1.75
2
κ

Figure 4

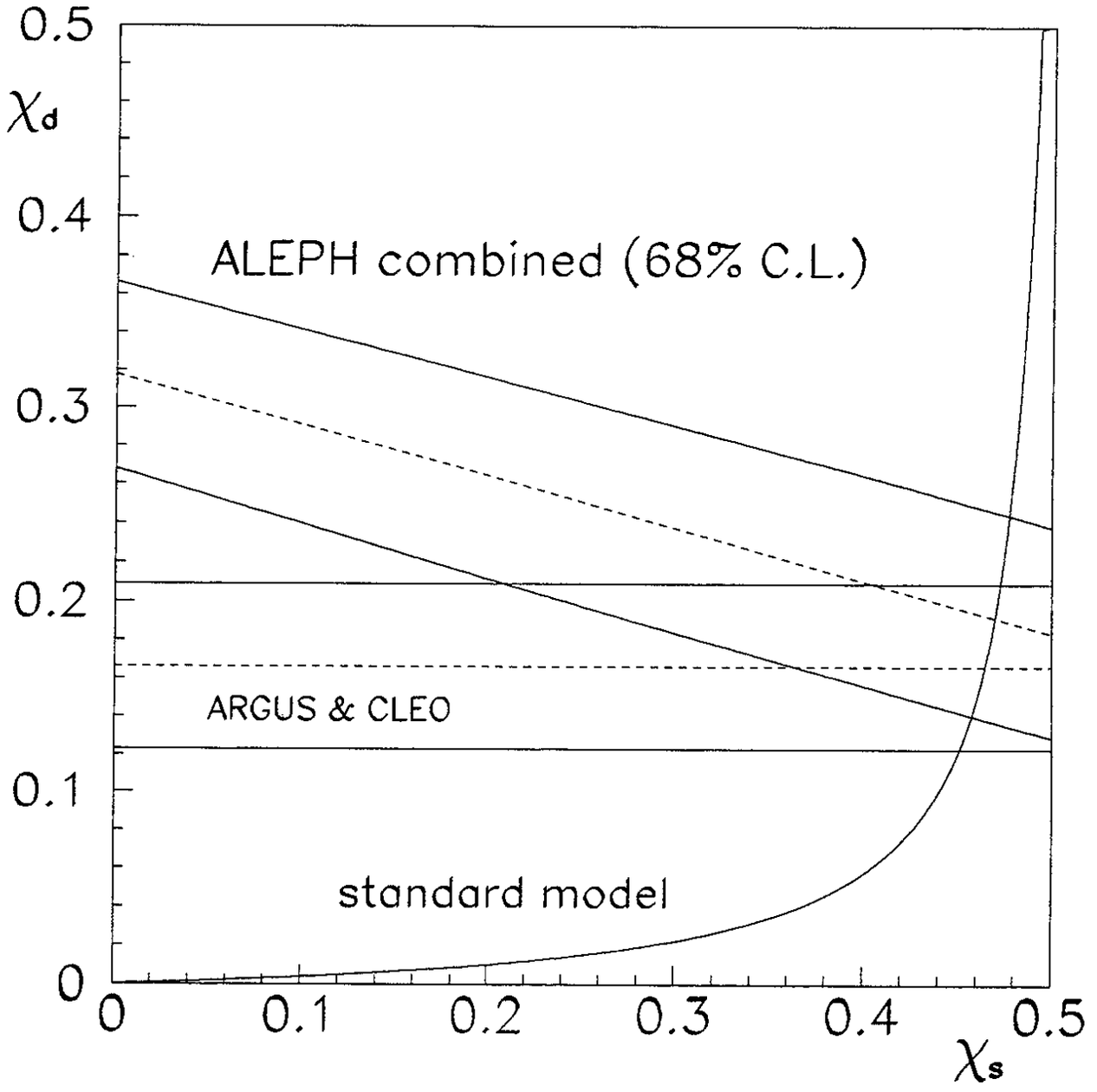
0.5
χ_d
0.4
ALEPH combined (68% C.L.)
0.3
0.2
ARGUS & CLEO
0.1
standard model
0
0
0.1
0.2
0.3
0.4
0.5
χ_s

Figure 5